Science Translational Medicine
AAAS

stm.sciencemag.org/cgi/content/full/11/500/eaav5464/DC1

Supplementary Materials for

Inhibition of natriuretic peptide receptor 1 reduces itch in mice

Hans Jürgen Solinski, Patricia Dranchak, Erin Oliphant, Xinglong Gu, Thomas W. Earnest, John Braisted, James Inglese, Mark A. Hoon*

*Corresponding author. Email: mark.hoon@nih.gov

Published 10 July 2019, *Sci. Transl. Med.* **11**, eaav5464 (2019)
DOI: 10.1126/scitranslmed.aav5464

The PDF file includes:

Other Supplementary Material for this manuscript includes the following:

(available at stm.sciencemag.org/cgi/content/full/11/500/eaav5464/DC1)

Data file S3 (Microsoft Excel format). qHTS follow-up screening data.
Data file S4 (Microsoft Excel format). Raw data.

Materials and Methods

Materials

Human NPPA, murine NPPA, and A-71915 were purchased from Bachem. Human NPPB, CYM5442 and Histamine were from Tocris, murine NPPB was from Peptide 2.0, and NPPC was from Mimotopes. JS-3 was purchased from Analyticon Biotechnologies, JS-4 – JS-10 were purchased from Charles River Discovery, JS-11 was from Chembridge, and JS-12 – JS-14 were from Chemdiv. If not indicated otherwise, all other reagents were purchased from ThermoFisher or Sigma-Aldrich.

In situ hybridization

DRGs from 4 different, healthy donors (see Table S9 for basic clinical data) were obtained from Tissue For Research (www.biobankonline.com) and the NIH NeuroBioBank at the University of Maryland (Baltimore, MD). Mouse DRGs were dissected from C57BL/6N mice (Envigo). ISH staining was performed using the RNAscope (ACD) technology according to the manufacturer's instructions. Probes specific for *hTRPV1*, *hNPPB*, *hTUBB3*, *hHRH1*, *hMRGPRX1*, *hIL31RA*, *mTrpV1*, and *mNppb* in conjunction with the RNAscope multiplex fluorescent development kit were used and nuclei were counter-stained using DAPI. Since human tissue has high auto-fluorescence, to quench auto-fluorescence after the staining procedure, DRG sections were consecutively treated with TrueView (Vector laboratories) and TrueBlack (Biotium). Images were collected on an Eclipse Ti (Nikon) confocal laser-scanning microscope using a 40X objective and to enhance visibility of the ISH signals, residual auto-fluorescent signal was background-subtracted with Image J (NIH). Estimation of soma-size

measurements was performed with ImageJ and plotted as a histogram with bins being identified by the respective lower limit.

Eukaryotic Expression Vectors

The vector pGS-40F, coding for a cGMP biosensor, and the vector pGS-22F, coding for a cAMP biosensor, were purchased from Promega. Expression vectors for murine and human NPR1, MC223390 and SC125506, respectively were purchased from OriGene Technologies. pDONR223-NPR2 (62) was a gift from William Hahn & David Root (Addgene plasmid # 23479) and the sequence coding for human NPR2 was sub-cloned into the expression vector pCMV6-Entry using standard molecular biology methodology. The generation of pEAK8-GFP was described previously (63).

Quantitative PCR

Total spinal cord RNA from 4 healthy donors (see Table S9 for basic clinical data) was obtained from the NIH NeuroBioBank at the University of Maryland (Baltimore, MD). Total RNA from human DRG (3 different, healthy donors, see Table S9), and mouse DRG and spinal cord was extracted using a RNeasy lipid tissue mini kit (Qiagen) following the manufacturer's instructions. During RNA extraction, on column DNAse treatment was performed. Total RNA was reverse transcribed using SMARTScribe reverse transcriptase (Takara Bio) and oligo(dT)18 primer according to the manufacturer's protocol. Exon-spanning gene-specific Taqman probes (*hNPPB*: 00173590, *hNPR1*: 00181445; *hGAPDH*: 02758991; *mNppb*: 01255770; *mNpr1*: 00435305; *mGapdh*: 99999915) in conjunction with Taqman gene expression master mix (all from ThermoFisher) were used to determine the expression of *NPPB* and *NPR1* on a MyIQ real-

time PCR machine (Bio-Rad). Cp values were called by the MyIQ software and the ΛCp method was used to calculate gene expression relative to the house-keeping control gene *GAPDH*.

Cell Culture and Transfection

HEK-293 cells (ATTC) were cultured in DMEM/F12 supplemented with 2 mM L-glutamine, 10% FBS, 100 U/ml penicillin, and 100 μg/ml streptomycin. For transient expression, 8 x 10^5 cells were seeded in 6-wells, cultured for 24 hours, and then transfected using TransIT-293 (Mirus Bio) according to the manufacturer's instructions. 48 hours after transfection, cells were used to measure intracellular cGMP (pGS-40F) or cAMP (pGS-22F) production. HEK-293 cell clones stably expressing pGS-40F alone (HEK-cGMP-sensor cells) or pGS-40F and human *NPR1* (HEK-hNPR1-cGMP-sensor cells) or pGS-40F and human *NPR2* (HEK-hNPR2-cGMP-sensor cells) were generated by co-transfection with pEAK8-GFP and selection with 1 μg/ml puromycin. Stable expression of transgenes was verified by measuring ligand-induced cGMP production with the cGMP biosensor.

Measurement of Intracellular cGMP Production Using the cGMP Biosensor pGS-40F

24 hours before measurements, 3 x 10^4 cells were seeded into white 96-well plates (PerkinElmer), coated with 0.1% poly(D-lysine), and assays conducted as recommended by the manufacturer (Promega). Briefly, media was aspirated and cells were loaded for two hours at room temperature with 2% GloSensor reagent diluted in CO_2-independent media supplemented with 2 mM L-glutamine and 10% FBS (assay medium). Luminescence was measured on a Synergy NEO plate reader (BioTek) at room temperature. After baseline measurement of 3-5 minutes, assay medium (as a control) or assay medium with agonist was manually added and luminescence was measured at ~1/60 Hz over 30 minutes. When compounds were tested for

NPR1/2 inhibition, compounds were added after baseline measurements and luminescence was read for 5 minutes before addition of agonist. Luminescence was normalized to baseline measurements and plotted. Ligand-induced changes of cGMP production were quantified by determining the area under the curve. To determine efficacy and potency of agonists, ligand-induced changes were normalized to vehicle addition and plotted against the ligand concentration. To quantify potency (IC_{50}) and efficacy (I_{max}) of compounds, compound-induced changes of agonist-induced cGMP production were normalized to vehicle controls, plotted against compound concentration, and fit with a four-parameter logistic regression. Effects of A-71915 on basal mNPR1 activity were fitted with a bell-shaped regression (equation indicated below). All fits were performed with Prism 7.0 (GraphPad).

Measurement of Intracellular cAMP Production Using the cAMP Biosensor pGS-22F

Intracellular cAMP production was measured as cGMP production with a few minor changes. Different concentrations of JS-11 or vehicle as a control were added to GloSensor reagent-loaded cells for 30 minutes before baseline cAMP amounts were measured for 5 minutes. Medium or medium containing forskolin (1 μM), to stimulate endogenously expressed ACs, was added and cAMP amounts measured for 30 minutes. Ligand-induced changes of cAMP production were quantified by determining the area under the curve and were expressed as forskolin-induced increase of cAMP over baseline amounts. Increases of cAMP amounts were plotted against JS-11 concentration to determine if JS-11 inhibited ACs.

LOPAC Validation of qHTS Assays

The Library of Pharmacologically Active Compounds (LOPAC) was used to validate the HEK-hNPR1-cGMP-sensor, HEK-hNPR2-cGMP-sensor and parental HEK-cGMP-sensor cell

lines for qHTS. The data for each can be found under PubChem AID 1347049, 1347050, 1347045, respectively or compiled in data file S1. The 1536-well generic plate map is shown in fig. S8, where controls for each assay are indicated in the legend.

Quantitative HTS

Measurement of intracellular cGMP production in HEK-hNPR1-cGMP-sensor cells was scaled to 4 µl volumes in 1536-well format and primary screening was performed in an automated manner in 7- to 11-point HTS. In short, 1.5 x 10^3 cells were plated in CO_2-independent assay medium in white, solid bottom TC treated 1536-well plates (Greiner Bio-One) with a multidrop combi dispenser. Cells were incubated at 37 ˚C, 5% CO_2 and 95% humidity for 16 hours and 1 µl of GloSensor reagent at a final assay concentration of 2% or assay medium as background control was added to respective wells with a BioRAPTR FRD (Beckman Coulter). Cells were incubated at room temperature for 2 hours, protected from light. 23 nl of compound were transferred by a pintool (Kalypsys) in the concentration range of 3.0 pM to 46.1 µM along with DMSO and a titration of A-71915 from 38.3 µM to 1.7 nM in columns 1-4 of each plate as vehicle and positive controls, respectively. Cells were incubated with compound for 30 minutes at room temperature. Pre-agonist luminescence for each plate was read on a ViewLux plate reader (PerkinElmer). 1 µl of hNPPA at a final assay concentration of 0.1 nM, or CO_2-independent media were added to respective wells with a BioRAPTR FRD. Plates were incubated for 20 min at room temperature, and luminescence was read on a ViewLux plate reader.

Pre-agonist and post-agonist data were normalized by plate to corresponding intra-plate controls as previously described (28). Assay statistics including S:N and Z' were calculated using the same respective controls. Pre-agonist data were normalized to the average signal of

DMSO-treated wells with 2% GloSensor reagent as 0% and the average signal of DMSO-treated wells with assay medium as -100% activity. Post-agonist data were normalized to the average signal of DMSO-treated wells with 2% GloSensor reagent and 0.1 nM hNPPA as 0% and the average signal of wells treated with 38.3 µM A-71915 with 2% GloSensor reagent and 0.1 nM hNPPA as -100% activity. The respective normalized data from each assay plate was corrected using DMSO only treated assay plates at the beginning and end of the screen and interspersed every 20-30 plates throughout screening. In-house software was used to fit the resulting inter-plate titration data to the standard hill equation and concentration-response curves were classified by activity as previously described (64). Curve fit assignments of 1.1, 1.2, 2.1, and 2.2 were considered active and visually confirmed. These data were refit in Prism 7.0 with nonlinear regression log(agonist) vs. response – variable slope (four parameters) fit. Bell-shaped curves were also fit in Prism 7.0 with nonlinear regression and the equation:

$$Y = S0 + \frac{(S1 - S0)}{(1 + 10^{((\log EC50 - X)*HillSlope\ 1)})} + \frac{(S2 - S1)}{(1 + 10^{((\log IC50 - X)*HillSlope\ 2)})}$$

Genesis Library Preparation

The Genesis collection is a novel chemical library with high quality chemotypes and core scaffolds amenable to rapid purchase and derivatization through medicinal chemistry. It consisted of 86,437 compounds at the time of screening. A minor subset of those compounds (~11,500) are part of a proprietary library and structures cannot be disclosed unless included in the follow-up selection. Library preparation and management were performed as previously described (65). Briefly, compounds were plated into 384-well plates (Greiner Bio-One) comprising a 7-point inter-plate titration with a serial dilution of 1:5 in dimethylsulfoxide

(DMSO) ranging from 10 mM to 640 µM. Plates were reformatted in quadrants into 1536-well format using an Evolution P3 system (PerkinElmer).

qHTS Follow-Up of Actives

From the 86,437 compounds tested in qHTS (PubChem AID 1347048 or data file S2), 1,408 compounds were selected to permit creation of a 1536-well inter-plate titration plate (65) for follow-up confirmation (the first 4-columns were reserved for assay controls, see fig. S8). Molecules were prioritized based on efficacy and potency in post-agonist concentration-response curves (curve classes -1.1, -1.2, -2.1, -2.2, see (28)). Molecules previously shown to directly inhibit *Firefly* luciferase ((66), PubChem AID 1347043) were subtracted from this group of molecules resulting in 1,336 compounds. Because 1,408 compounds can efficiently be tested simultaneously in a 1536-well inter-plate titration, the 72 highest potency, lower quality qHTS curve class actives (-2.4) were added to bring the number of compounds for re-testing to 1,408. Activity of compounds on non-stimulated cells (pre-agonist data) was not considered for prioritization. Compounds selected for follow-up were re-plated in 11-pt inter-plate titration with a serial dilution of 1:3 in DMSO ranging from 10 mM to 169 µM. The primary screening assay was repeated with the follow-up compounds as described above (1,382 compounds were reconfirmed, PubChem AID 1347044 or data file S3). In addition, counter-screens were performed with HEK-hNPR2-cGMP-sensor and HEK-cGMP-sensor cells. These cells were stimulated with 1 nM NPPC or 50 µM SNP, respectively, but otherwise the assay was conducted as described for HEK-hNPR1-cGMP-sensor cells. Pre-agonist controls were the same for all three assays, but normalization of post-agonist data differed between assays. For HEK-hNPR1-cGMP-sensor cells, normalization was carried out as described for primary screening, whereas for HEK-hNPR2-cGMP-sensor and HEK-cGMP-sensor cells, the average signal of DMSO-

treated wells with 2% GloSensor reagent without and with the respective agonist were defined as -100% or 0% activity, respectively and data were normalized accordingly.

Cytotoxicity Counter-Screen

A cytotoxicity counter-screen using HEK-hNPR1-cGMP-sensor cells was performed on the follow-up compounds, as previously described (30). Briefly, 1.5 x 10^3 cells were plated in 4 µL CO_2-independent assay media in white, solid bottom TC-treated 1536-well plates (Greiner Bio-One) as above. Cells were incubated at 37 ˚C, 5% CO_2 and 95% humidity for 16 hours, compound transfer was performed as described for qHTS along with DMSO and a titration of Digitonin from a top concentration of 115 µM to 3.5 nM in columns 1-4 of each assay plate as vehicle and cytotoxicity controls, respectively. Cells were incubated with compound for 2 hours at 37 ˚C. 3 µl of CellTiter-Glo reagent (Promega) were added to each well with a BioRAPTR FRD and plates were incubated for 10 min at room temperature, protected from light. Luminescence was measured on a ViewLux plate reader. Data were normalized to the average signal of DMSO-treated wells as 0% and the average signal of wells treated with 115 µM Digitonin as -100% activity and analyzed as above.

Biochemical *Firefly* Luciferase Enzymatic Counter-Screen

A *Firefly* luciferase enzyme assay was performed at Km on the follow-up compounds as previously described (30). In brief, 3 µl of substrate-buffer solution (0.01 mM D-Luciferin, 0.01 mM ATP, 50 mM Tris Acetate, 10 mM Mg Acetate, 0.01% Tween-20 and 0.038% BSA final concentrations) were dispensed into white, solid bottom medium bind 1536-well plates (Greiner Bio-One) with a BioRAPTR FRD. Compounds were transferred as described for qHTS along with DMSO and titrations of PTC124 ranging from top concentration 57.5 µM to 4.0 pM in

columns 1-4 of each plate as vehicle and positive controls, respectively. 1 µl luciferase enzyme-buffer solution (10 nM P. *pyralis* luciferase in 50 mM Tris Acetate final concentration) was dispensed and, after a 5-minute incubation at room temperature, luminescence was read on a ViewLux plate reader. Data were normalized to DMSO-treated wells as 0% and the average signal of wells treated with 57.5 µM PTC124 as -100% activity and processed as above.

Selection of JS-1 through JS-15 after follow-up counter-screening

Of the 1,382 reconfirmed follow-up compounds, compounds with similar or higher curve class values in HEK-cGMP-sensor cells (PubChem AID 1347051 or data file S3) were removed from further consideration. Additionally, curve classes of -1.1, -1.2, -2.1, or -2.2 observed in the cytotoxicity counter-screen, measured in HEK-hNPR1-cGMP-sensor cells (PubChem AID 1347044 or data file S3), and in the biochemical *Firefly* luciferase enzymatic counter-screen (PubChem 1347047 or data file S3) reduced the compounds of interest to 149. From these, only 15 compounds, named JS-1 – JS-15, were selected for further pharmacological evaluation, based on the visual inspection of concentration response curves (fig. S9). Of note, none of these molecules displayed hNPR1 selectivity over hNPR2 (PubChem AID 1347046 or data file S3).

SafetyScreen44

SafetyScreen44 was used to identify potential off-target effects of JS-11. Each target was tested for inhibition by 10 µM JS-11 in duplicate by Eurofins Panlabs Discovery Services Taiwan. Significant inhibition of targets was accepted at ≥ 50% inhibition. See table S3 for detailed information on target selection and methodology used to measure inhibition of target activity.

Membrane Fractionation

Membranes were fractioned from HEK-hNPR1-cGMP-sensor cells grown for 2 days to confluence on 150 mm plates (seeded with 8 x 10^6 cells). Medium was aspirated and cells were washed with ice-cold phosphate-buffered saline (PBS) without Ca^{2+}/Mg^{2+}. Cells were scraped loose in ice-cold 2.5 ml homogenization buffer (50 mM HEPES, 5 mM EDTA, 50 mM NaCl, 50 mM NaF, 250 nM microcystin, 20% glycerol, cOmplete ULTRA Mini protease inhibitor cocktail) with a rubber policeman and lysed with a glass-Teflon homogenizer on ice. To remove debris, the lysate was spun for 10 minutes at 500 x g and 4 ˚C. While the supernatant was stored on ice, the pellet was lysed again with a glass-Teflon homogenizer and centrifuged again for 10 minutes at 500 x g and 4 ˚C. Both supernatants were pooled and spun for 60 minutes at 100,000 x g and 4 ˚C in a XL-90 ultracentrifuge (Beckman Coulter) equipped with a 70-Ti rotor. The supernatant was discarded and the pellet was resuspended in membrane buffer (10 mM HEPES, 1 mM EDTA, 250 nM microcystin, cOmplete Ultra Mini protease inhibitor cocktail) by passing multiple times through a 25ga needle. Protein content of membrane fractions was assessed by BCA assay according to the manufacturer's instructions. Membranes were aliquoted to 100 µg protein, flash frozen in liquid nitrogen, and stored at -80 ˚C.

Measurement of NPR1 Enzymatic Activity in Membrane Fractions

For measurement of hNPR1 cyclase activity, 2 µg of membranes were diluted to 20 µl with H_2O and mixed with 2.5 µl NPR1 antagonist (at the concentrations indicated in figures) and incubated for 5 minutes. The enzymatic reaction was initiated by the addition of pre-warmed 25 µl 2-fold concentrated assay buffer (25 mM HEPES, 1 mM EDTA, 1 mM ATP, 5 mM $MgCl_2$, 500 µM microcystin, 2 mM GTP final concentrations) with and without hNPPA and incubated at 37 ˚C for 5 minutes. Reactions were stopped by addition of 19.3 µl 1 M hydrochloric acid and

mixed on a shaker for 10 minutes. Samples were diluted appropriately and analyzed for cGMP content using a competitive colorimetric immunoassay (ADI-901-014, Enzo Life Sciences) according to the manufacturer's instructions. To account for differences in cGMP content of starting material, a mock reaction that lacked the substrate GTP was performed and subtracted from experimental samples. To quantify efficacy (IC_{50}) and potency (I_{max}) of compounds, compound-induced changes of agonist-induced cGMP production were normalized to vehicle controls, plotted against the compound concentration, and data was fit with Prism 7.0 using a four-parameter logistic regression.

Kinetic Solubility Assay

The µSOL assay was used for kinetic solubility determination (67). In this assay, the classical saturation shake-flask solubility method was adapted as previously described (67). Test compounds were prepared as 10 mM DMSO stock solutions and diluted to a final compound concentration of 150 µM in aqueous solution (pH 7.4, 100 mM phosphate buffer). Samples were incubated at room temperature for 6 hours and vacuum-filtered using Te-Vac (Tecan) to remove any precipitates. The concentration of the compound in the filtrate was measured via UV absorbance (λ: 250-498 nm). The unknown compound concentration was determined by comparison to the fully solubilized reference plate which contained 17 µM of compound dissolved in spectroscopically pure n-propanol. All compounds were tested in duplicates. The kinetic solubility (µg/ml) of compounds was calculated using the µSOL Evolution software (Pion Inc.). The three controls used were albendazole (low solubility), phenazolpyridine (moderate solubility) and furosemide (high solubility).

Rat Liver Microsome Stability Assay

Single time point microsomal stability was determined in a 96-well HTS format. Sample preparation was automated using an EVO 200 robot (Tecan). A high-resolution LC/MS (Thermo QExactive) instrument was used to measure the percentage of compound remaining after incubation using a previously described method (68). Six standard controls were tested in each run: buspirone and propranolol (for short half-life), loperamide and diclofenac (for short to medium half-life), and carbamazepine and antipyrine (for long half-life). Briefly, the incubation consisted of 0.5 mg/ml microsomal protein, 1.0 μM compound concentration, and NADPH regeneration system (containing 0.650 mM $NADP^+$, 1.65 mM glucose 6-phosphate, 1.65 mM $MgCl_2$, and 0.2 U/mL G6PDH) in 100 mM phosphate buffer at pH 7.4. The incubation was carried out at 37 °C for 15 min. The reaction was quenched by adding 555 μl of acetonitrile (∼1:2 ratio) containing 0.28 μM albendazole (internal standard).

Parallel Artificial Membrane Permeability Assay (PAMPA)

Stirring double-sink PAMPA method was employed to determine the permeability of compounds via PAMPA. The PAMPA lipid membrane consisted of an artificial membrane of a proprietary lipid mixture and dodecane (Pion Inc.), optimized to predict gastrointestinal tract passive permeability. The lipid was immobilized on a plastic matrix of a 96-well "donor" filter plate placed above a 96-well "acceptor" plate. pH 7.4 solution was used in both donor and acceptor wells. The test articles, stocked in 10 mM DMSO solutions, were diluted to 0.05 mM in aqueous buffer (pH 7.4), and the concentration of DMSO was 0.5% in the final solution. During the 30-minute permeation period at room temperature, the test samples in the donor compartment were stirred using the Gutbox technology (Pion Inc.) to reduce the aqueous boundary layer. The test article concentrations in the donor and acceptor compartments were measured using an UV

plate reader (Nano Quant, Infinite 200 PRO, Tecan). Permeability calculations were performed using Pion Inc. software and were expressed in units of 10^{-6} cm/s. Compounds with low or weak UV signal were analyzed using high resolution LC/MS (Thermo QExactive).

Behavioral Measurement of Acute Scratching Behavior

All experiments using mice followed NIH guidelines and were approved by the National Institute of Dental and Craniofacial Research ACUC. Behavioral assessment of scratching behavior was conducted as described previously (69). Briefly, 6-8-week old female C57BL/6N mice (Envigo) were injected intraperitoneally with JS-11 (163 μg) or DMSO (20%) as a vehicle control or intrathecally with JS-11 (16.3 μg) or DMSO (20%) as a vehicle control, following a cross-over design. 10 minutes later, 100 μg histamine diluted in 10 μl PBS or 8.9 μg CYM5442 diluted in 10 μl ddH_2O was injected subcutaneously into the nape of the neck. Note that consecutive injections were 2 weeks apart. Scratching behavior was recorded for 30 minutes and is presented in bouts per 30 minutes. One bout was defined as scratching behavior towards the injection site between lifting the hind leg from the ground and either putting it back on the ground or guarding the paw with the mouth.

Behavioral Measurement of Chronic Scratching Behavior

The contact hypersensitivity model was performed as previously described (42). Briefly, the back of 6-8-week old female C57BL/6N mice (Envigo) was shaved with electric clippers. After 2 days, 25 μl of 0.5% (v/v) dinitro-fluoro-benzene (DNFB) diluted in a 4:1 mixture of acetone and olive oil was applied to the shaved back skin. Hapten challenge was performed 5 days after sensitization by applying 40 μl of 0.2% (v/v) DNFB in the same vehicle on the left ear and 40 μl of vehicle alone on the right ear. After 24 hours, baseline scratching was observed for

30 minutes. Mice were then injected intraperitoneally with JS-11 (163 μg) or DMSO (20%) as a vehicle control. After 10 minutes, scratching was again observed for 30 minutes. To assess skin inflammation, ear thickness was measured with a thickness gauge (Mitutoyo, Aurora, IL) before and 30 minutes after JS-11/DMSO injections and normalized to ear thickness before hapten challenge. Note that hapten challenge (left ear) induced significantly more skin inflammation than application of vehicle alone (right ear) (DMSO group: left ear 191.7 ± 8.4%, right ear 119.7 ± 6.5%, $p = 0.0002$; JS-11 group: left ear 194.2 ± 12.1%, right ear 120.1 ± 6.1%, $p = 0.0004$; both repeated-measure ANOVA with Sidak's multiple comparisons post-hoc test). For visualization, scratching bouts and ear thickness for each mouse were normalized to baseline values (100%) and plotted.

Measurement of Effects on Locomotion

To control for motor impairment by JS-11, rotarod performance was assessed 10 minutes after intraperitoneal injection of JS-11 (163 μg) or DMSO (20%) as vehicle control, using a previously described method (70). A total of 10 C57BL/6N mice (Envigo) were analyzed in a cross-over design. Note that consecutive injections were 2 weeks apart. As a second measure of effects on locomotion, spontaneous locomotor activity was measured in the home cage by telemetry. In 5 C57BL/6N mice, chronically implanted with a telemeter (71), locomotor activity was measured (1/60 Hz) for 1 hour before and 3 hours after intra-peritoneal injection of JS-11 (163 μg) or DMSO (20%) as vehicle control, following a cross-over design. Note that consecutive injections were 1 week apart. Cumulative spontaneous locomotor activity (area under the curve (AUC)) in the first hour post injection was quantified for each mouse to compare treatment groups.

Measurement of Pharmacokinetics in Vivo

6-8-week old female C57BL/6N mice (Envigo) were injected with JS-11 (5 mg/kg) and sacrificed at different time points after injection. For each time point, three animals were dosed. Blood was collected by cardiac puncture into K_2EDTA tubes (BD) and centrifuged for 10 minutes at 1,500 x g and 4 ˚C. Plasma was transferred to a new tube and kept at -80 ˚C until analysis. Brains from the same mice were dissected, snap frozen in liquid nitrogen and kept at -80 ˚C until analysis. The drug concentrations in plasma and brain homogenate were determined with a qualified UPLC-MS/MS method with an Acquity UPLC and Xevo TQ-S system (Waters). The Acquity UPLC BEH C18 column (1.7 µm, 2.1 ID X 50 mm length) was used. The mobile phase consisted of 0.1% formic acid in water (Solvent A) and 0.1% formic acid in acetonitrile (Solvent B), and the flow rate was 0.6 ml/min. Pharmacokinetic characteristics were calculated using the non-compartmental approach (model 200) with Phoenix WinNonlin (Certara). JS-11 concentrations were plotted against time and the slope of the apparent terminal phase was estimated by log linear regression using at least 3 data points. The terminal rate constant (λ) was derived from this slope. The apparent terminal half-life ($t_{1/2}$) was calculated as $0.693/\lambda$. The area under the concentration-time curve, estimated as the sum of the $AUC_{0-4\,h}$ (the time of the last measurable concentration) plus Ct/λ, was used to calculate the concentration ratio of JS-11 in brain and plasma.

Measurement of Cardiovascular Effects

6-8-week old female C57BL/6N mice (Envigo) were anesthetized with 2-3% isoflurane and kept warm using a water blanket. The body temperature was monitored using a rectal thermometer and maintained between 36.7 and 37.3 ˚C throughout the procedure. While under anesthesia, an incision was made midline in the throat and the right carotid artery was isolated

and cannulated using a 1F solid state catheter (Millar Instruments). Blood pressure and heart rate were measured (~5 Hz) at baseline and for 45 minutes following intra-peritoneal injection of either JS-11 (163 μg) or DMSO (20%) as vehicle control. The data was collected and analyzed using PowerLab hardware and LabChart software (ADInstruments). Data was averaged in 2 second bins and across treatment (5 animals each) and mean blood pressure (average of systolic and diastolic blood pressure) and heart rate were plotted against the time to visualize overall time-dependent effects. Three epochs (baseline, first 5 minutes post injection, and 5-40 minutes post injection) were defined and minimum and maximum as well as average data (AUC/min) were extracted from each epoch to compare treatment groups.

Immunohistochemical Measurement of c-FOS Induction in Spinal Cord Neurons

c-FOS induction was measured as described previously with a few modifications (34). Briefly, the lateral thigh of 6-8-week C57BL/6N mice of either sex was shaved 24 hours prior to intradermal injection of histamine (100 μg in 10 μl saline). To prevent noxious stimulation of the injection site due to biting, mice wore an Elizabethan collar. 2 hours post injection, mice were trans-cardially perfused with paraformaldehyde (PFA, 4 %) before the lumbar spinal cord (L3-L4) was dissected and post-fixed overnight in PFA. The contralateral side was notched to identify the injection site. Tissue was cryo-protected in sucrose (30%) before being cryo-sectioned at 40 μm. Free-floating sections were incubated overnight at room temperature in rabbit anti-c-FOS monoclonal antibody (9F6, Cell Signaling Technology), diluted 1:50 in PBS/0.1% Triton-X-100 (PBS/T). After 3 washes in PBS/T, sections were incubated in Alexa Fluor488-conjugated donkey-anti-rabbit secondary antibody (711-545-152, Jackson ImmunoResearch), diluted 1:500 in PBS/T for 75 minutes at room temperature. After 3 washes in PBS/T, sections were mounted on glass slides in Fluoromount G with DAPI

(SouthernBiotech) and imaged on an Eclipse Ti (Nikon) confocal laser-scanning microscope with appropriate filter sets. The number of c-FOS positive cells in the dorsal spinal cord, ipsilateral and contralateral to the injection site, were quantified with Image J (NIH) by an observer blind to the treatment. 6 sections covering the area with the most intense induction of c-FOS were counted. A total of 8 mice, 4 per treatment group were analyzed.

Figure S1

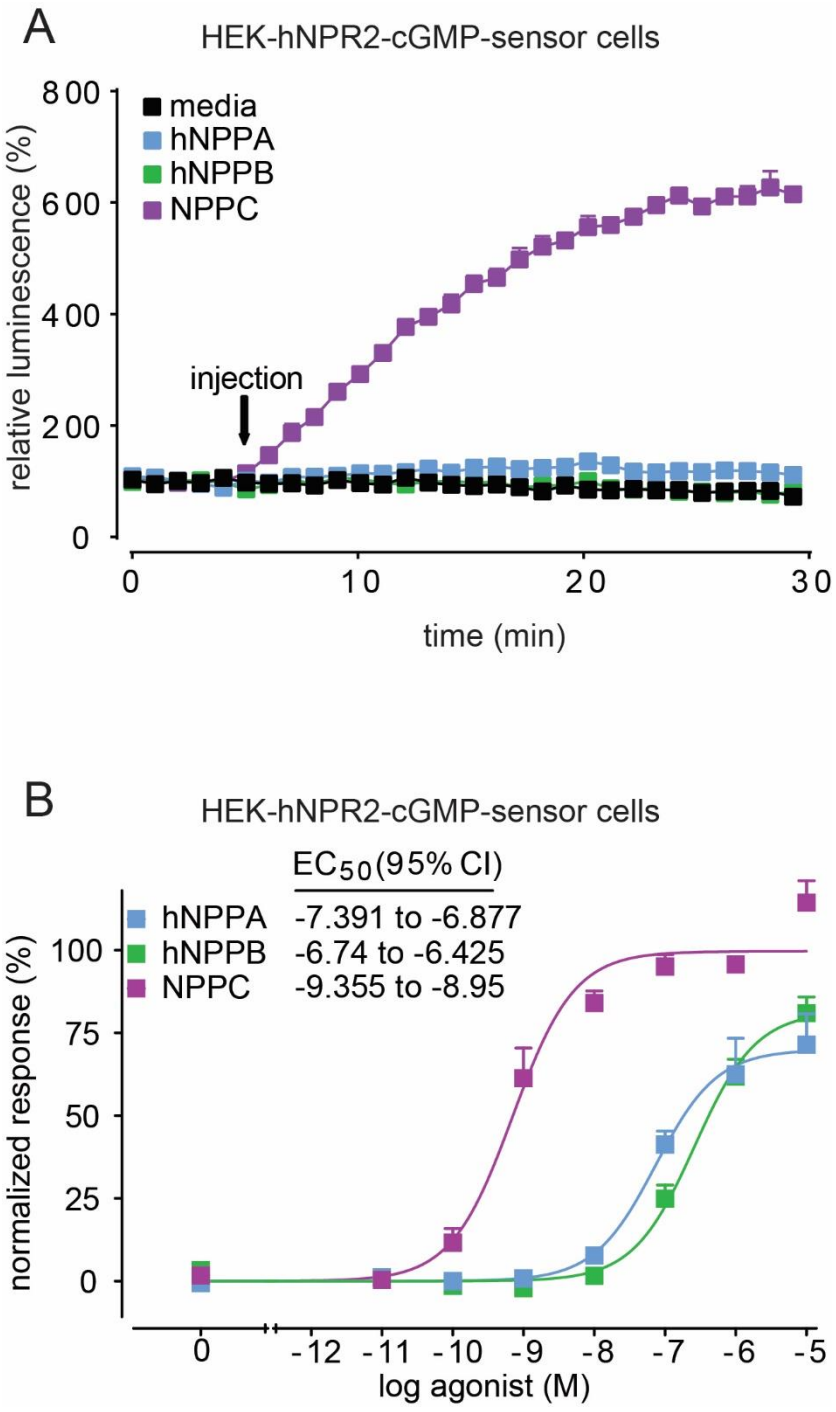
A
HEK-hNPR2-cGMP-sensor cells
media
hNPPA
hNPPB
NPPC
injection
relative luminescence (%)
800
600
400
200
0
0
10
20
30
time (min)
B
HEK-hNPR2-cGMP-sensor cells
EC50(95% CI)
hNPPA -7.391 to -6.877
hNPPB -6.74 to -6.425
NPPC -9.355 to -8.95
normalized response (%)
100
75
50
25
0
0
-12
-11
-10
-9
-8
-7
-6
-5
log agonist (M)

Fig. S1. Generation of HEK-hNPR2-cGMP sensor cells.

(A) Quantification of the specificity of cloned stable cell-line expressing pGS-40F with hNPR2 (HEK-hNPR2-cGMP-sensor cells). Time course measurements of luminescence produced by activation of hNPR2 with media (black), hNPPA (blue), hNPPB (green), and NPPC (purple). (B) Quantification of activity of HEK-hNPR2-cGMP-sensor cells to hNPPA (blue), hNPPB (green), and NPPC (purple). Data represent duplicate (A) or triplicate (B) measurements.

Figure S2

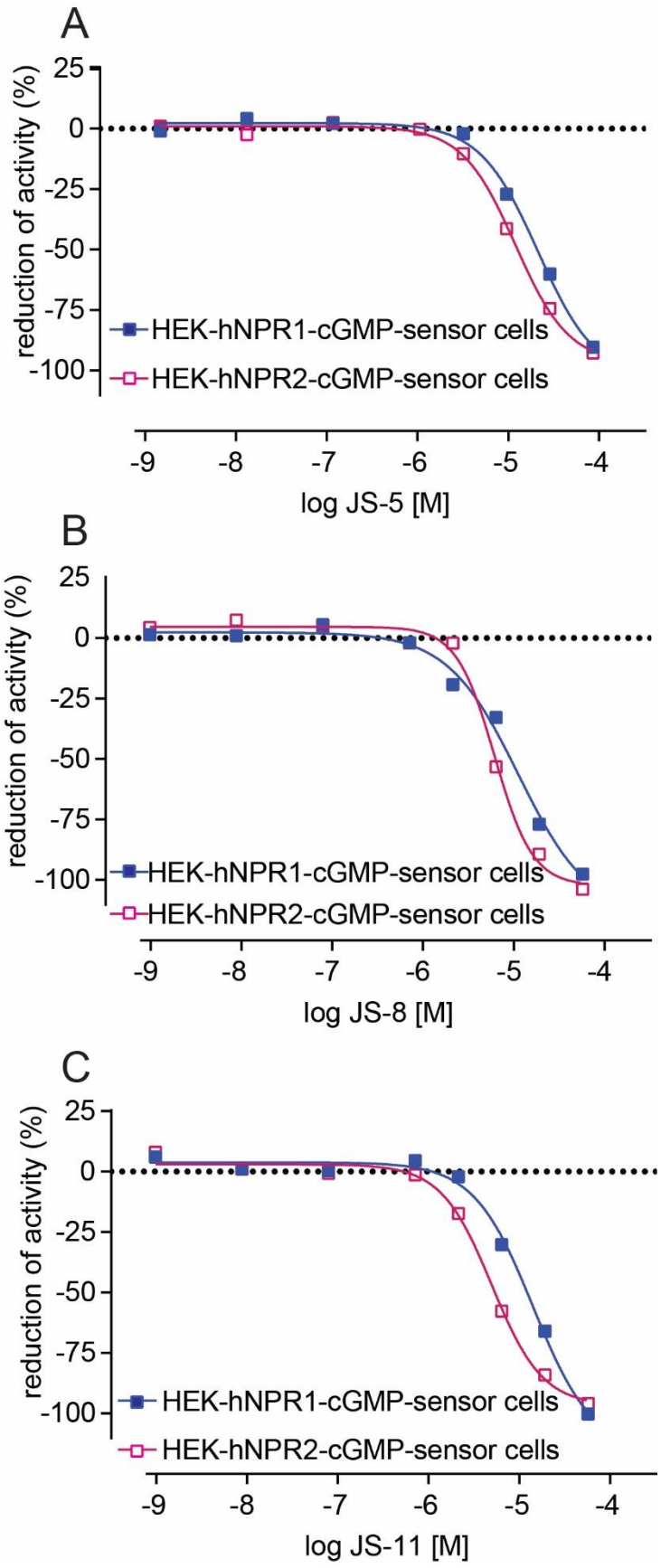
A
reduction of activity (%)
25
0
-25
-50
-75
-100
HEK-hNPR1-cGMP-sensor cells
HEK-hNPR2-cGMP-sensor cells
-9
-8
-7
-6
-5
-4
log JS-5 [M]
B
reduction of activity (%)
25
0
-25
-50
-75
-100
HEK-hNPR1-cGMP-sensor cells
HEK-hNPR2-cGMP-sensor cells
-9
-8
-7
-6
-5
-4
log JS-8 [M]
C
reduction of activity (%)
25
0
-25
-50
-75
-100
HEK-hNPR1-cGMP-sensor cells
HEK-hNPR2-cGMP-sensor cells
-9
-8
-7
-6
-5
-4
log JS-11 [M]

Fig. S2. hNPR1 inhibitors also block hNPR2.

Quantification of the reduction of hNPR1 (blue squares) and hNPR2 (red open squares) activity by JS-5 (A), JS-8 (B), and JS-11 (C). Data were collected from qHTS assays.

Figure S3

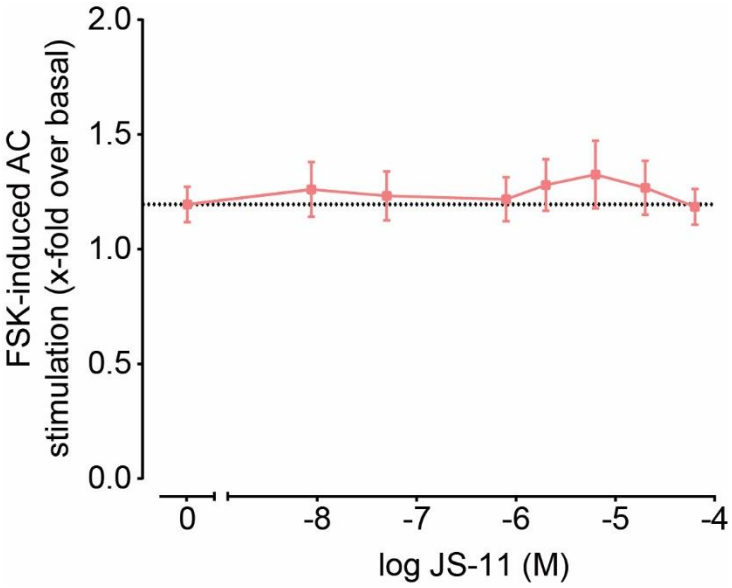

Fig. S3. JS-11 does not inhibit ACs.

Quantification of modulation by JS-11 of forskolin (FSK)-induced stimulation of AC activity in HEK-293 cells. Data represent means of ± SEM of 4 independent experiments.

Figure S4

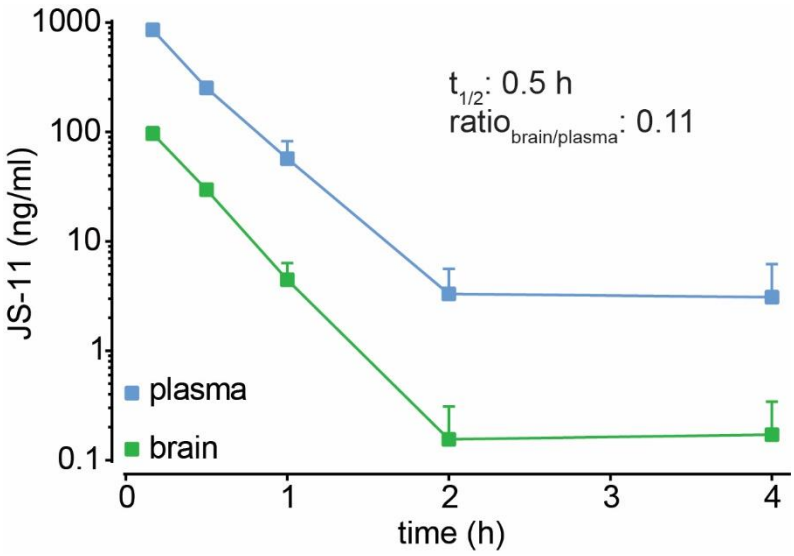

Fig. S4. In vivo pharmacokinetics of JS-11.

Quantification of the time-course of clearance of JS-11 in mice (intra-peritoneal injection (5 mg/kg)). Concentrations of JS-11 were quantified in plasma (blue) and brain tissue (green) by UPLC-MS/MS and used to calculate the ratio of cumulative JS-11 amounts in brain and plasma. Data represent means ± SEM (n=3 mice per time point).

Figure S5

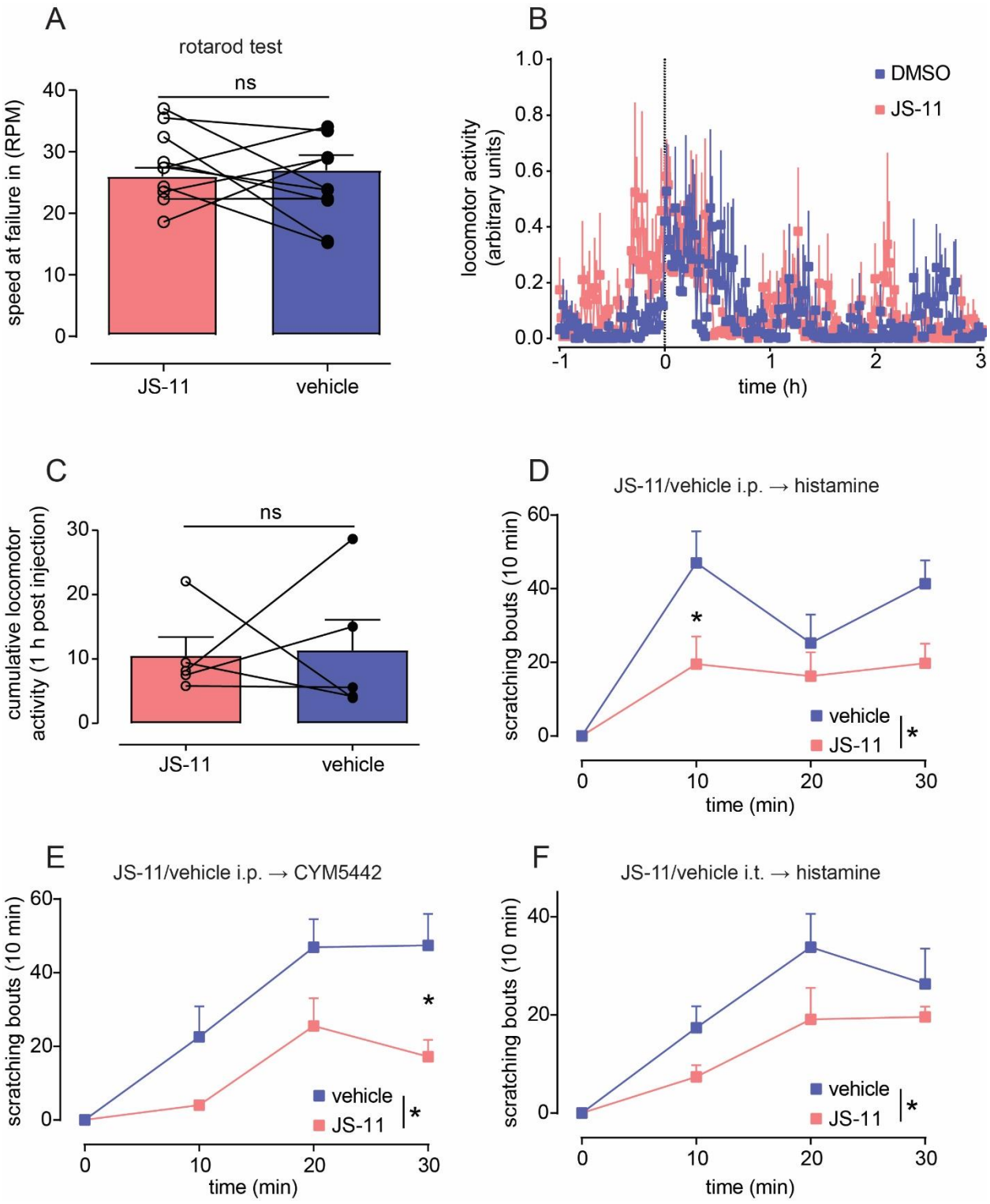
A
rotarod test
ns
speed at failure in (RPM)
40
30
20
10
0
JS-11
vehicle
B
DMSO
JS-11
locomotor activity (arbitrary units)
1.0
0.8
0.6
0.4
0.2
0.0
-1
0
1
2
3
time (h)
C
ns
cumulative locomotor activity (1 h post injection)
30
20
10
0
JS-11
vehicle
D
JS-11/vehicle i.p. → histamine
scratching bouts (10 min)
60
40
20
0
*
vehicle
JS-11
*
0
10
20
30
time (min)
E
JS-11/vehicle i.p. → CYM5442
scratching bouts (10 min)
60
40
20
0
*
vehicle
JS-11
*
0
10
20
30
time (min)
F
JS-11/vehicle i.t. → histamine
scratching bouts (10 min)
40
20
0
vehicle
JS-11
*
0
10
20
30
time (min)

Fig. S5. Effects of NPR1 antagonist on general motor behavior and itch responses. (A) Quantification of effects on motor coordination of administration of JS-11 (163 μg) using an accelerating rod assay. JS-11 (pink) did not significantly alter the speed for failure compared to vehicle control (blue; 20% DMSO) (ns P = 0.6539, paired t-test). (B-C) Quantification of effects on spontaneous locomotor activity of administration of JS-11 (163 μg). (B) Time-course data from 1 hour prior to 3 hours after injection of JS-11 are shown. (C) Cumulative spontaneous activity in the first hour after injection was quantified. JS-11 (pink) did not significantly alter spontaneous activity compared to vehicle control (blue) (ns P > 0.9999, Wilcoxon test). (D-F) Quantification of data from Fig. 7B,C,G plotting itch responses over a time course with epochs of 10 minutes. Differences in itch responses to JS-11- (pink) and vehicle-treated (blue) mice were analyzed using 2-way ANOVA (D, *P = 0.0017; E, *P = 0.001; F, *P = 0.02). Sidak's multiple comparisons post-hoc test was used to assess differences at each timepoint (D, 10 min: *P = 0.0262, 20 min: ns P = 0.7542, 30 min: ns P = 0.1054; E, 10 min: ns P = 0.1681, 20 min: ns P = 0.0902, 30 min: *P = 0.0085; E, 10 min: ns P = 0.4673, 20 min: ns P = 0.1602, 30 min: ns P = 0.7576). Data represent means $\pm$ SEM (n=10 (A and E), n=8 (D and F), and n=5 (B and C) animals per treatment group.

Figure S6

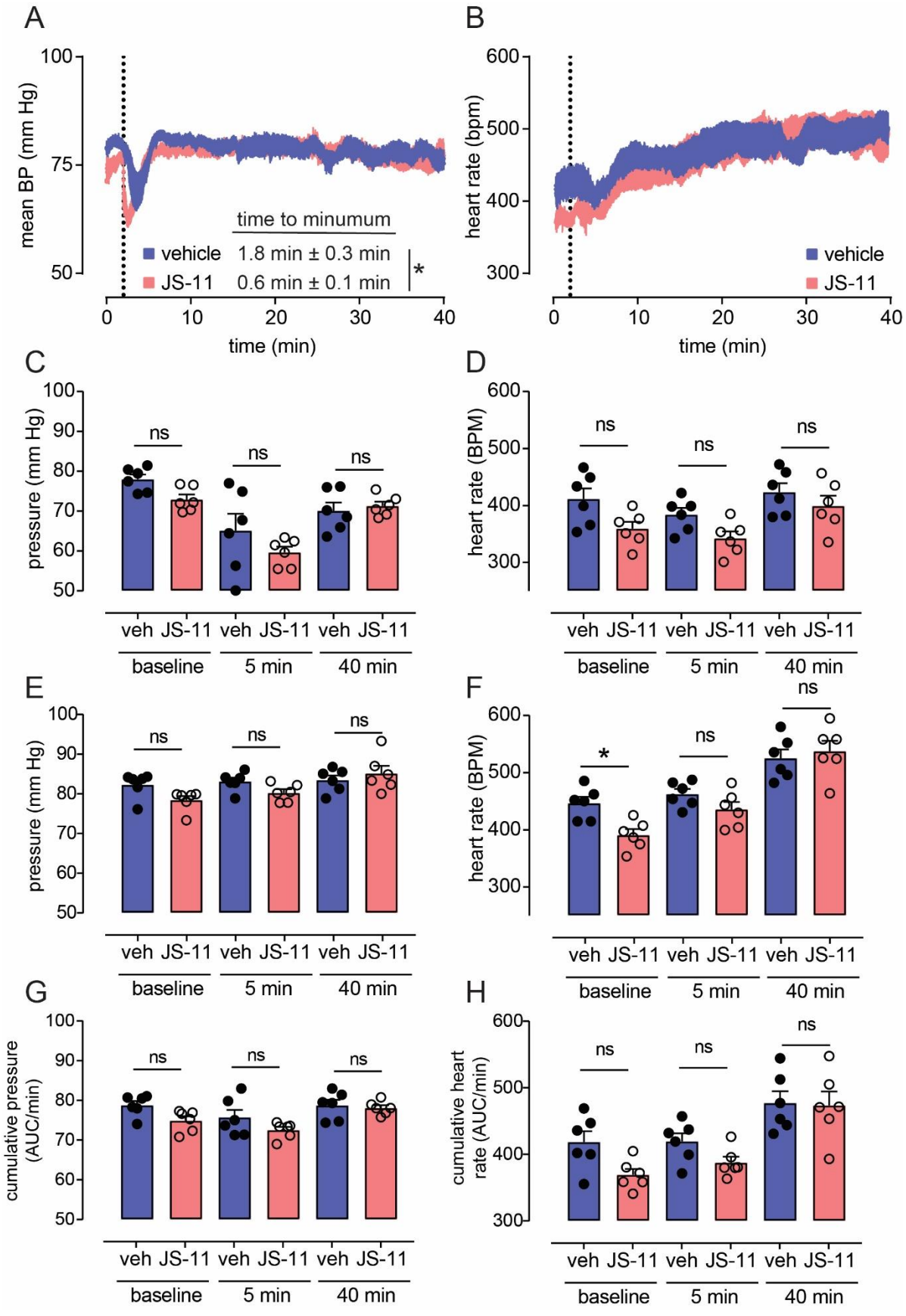
A
mean BP (mm Hg)
time to minumum
vehicle 1.8 min ± 0.3 min
JS-11 0.6 min ± 0.1 min
*
time (min)
B
heart rate (bpm)
vehicle
JS-11
time (min)
C
pressure (mm Hg)
D
heart rate (BPM)
E
pressure (mm Hg)
F
heart rate (BPM)
G
cumulative pressure (AUC/min)
H
cumulative heart rate (AUC/min)
ns
*
veh JS-11 veh JS-11 veh JS-11
baseline
5 min
40 min

Fig. S6. JS-11 does not cause extensive cardiovascular side effects.

Quantification of blood pressure (A) and heart rate (B) at baseline (left of dotted line) and for 40 minutes post administration of JS-11 (pink; intraperitoneal injection, 163 μg) or vehicle (blue; 20% DMSO). For both treatment groups there was a transient, but reversible, drop in blood pressure, with JS-11 causing slightly faster kinetics (unpaired t-test, p = 0.0042). Quantification of effects on blood pressure (C, E, G) and heart rate (D, F, H), minimum (C,D), maximum (E,F) and average (AUC/minute, G,H) were analyzed for three epochs (baseline, first 5 minutes post injection, and 5-40 minutes post injection). Between treatment groups, differences were determined with 1-way ANOVA and Sidak's multiple comparisons post-hoc test (C, baseline: ns P = 0.3076, 5 min: ns P = 0.2481, 40 min: ns P = 0.9713; D, baseline: ns P = 0.0582, 5 min: ns P = 0.1705, 40 min: ns P = 0.5996; F, baseline: *P = 0.0167, 5 min: ns P = 0.4188, 40 min: ns P = 0.8873; G, baseline: ns P = 0.1017, 5 min: ns P = 0.2233, 40 min: ns P = 0.9774; H, baseline: ns P = 0.0812, 5 min: ns P = 0.3766, 40 min: ns P = 0.9977) or Friedman test with Dunn's multiple comparisons post-hoc test (E, baseline: ns P = 0.1346, 5 min: P = 0.4947, 40 min: P > 0.9999). The maximum and average but not minimum heart rate increased significantly over the time of the experiment in both treatment groups (repeated measure ANOVA with Tukey's multiple comparisons post-hoc test, minimum vehicle: ns P = 0.6121; minimum JS-11: ns P = 0.1021; maximum vehicle: *P = 0.0078; maximum JS-11: *P < 0.0001; average vehicle: *P = 0.0226; average JS-11: *P = 0.0013). Data represent means $\pm$ SEM (n=6 animals per treatment group).

Figure S7

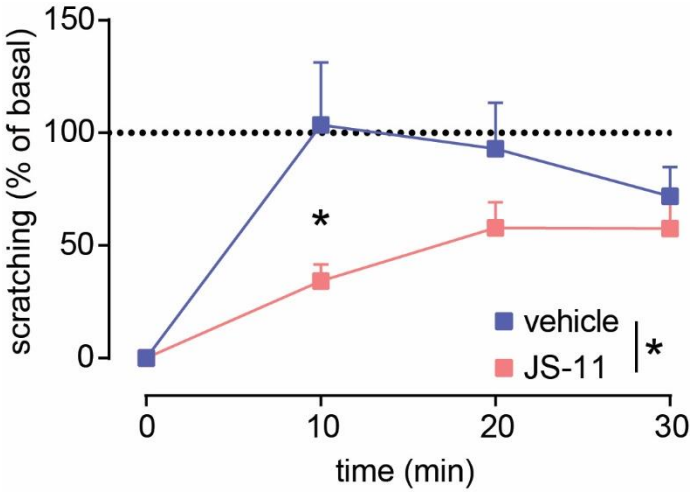

Fig. S7. JS-11 inhibits itching in a mouse model of contact dermatitis. Quantification of data from Fig. 8D plotting itch responses in 10-minute epochs. Changes of scratching were normalized to baseline activity (100%, dotted line) and differences in itch responses to JS-11- (163 μg, intraperitoneal injection, pink) and vehicle-treated (20% DMSO, blue) mice were analyzed using 2-way ANOVA (*P = 0.006). Sidak's multiple comparisons post-hoc test was then used to more specifically assess differences at each timepoint (10 min: *P = 0.0165; 20 min: ns P = 0.3851; 30 min: ns P = 0.9096). Data represent means ± SEM (n=10 animals per treatment group).

Figure S8

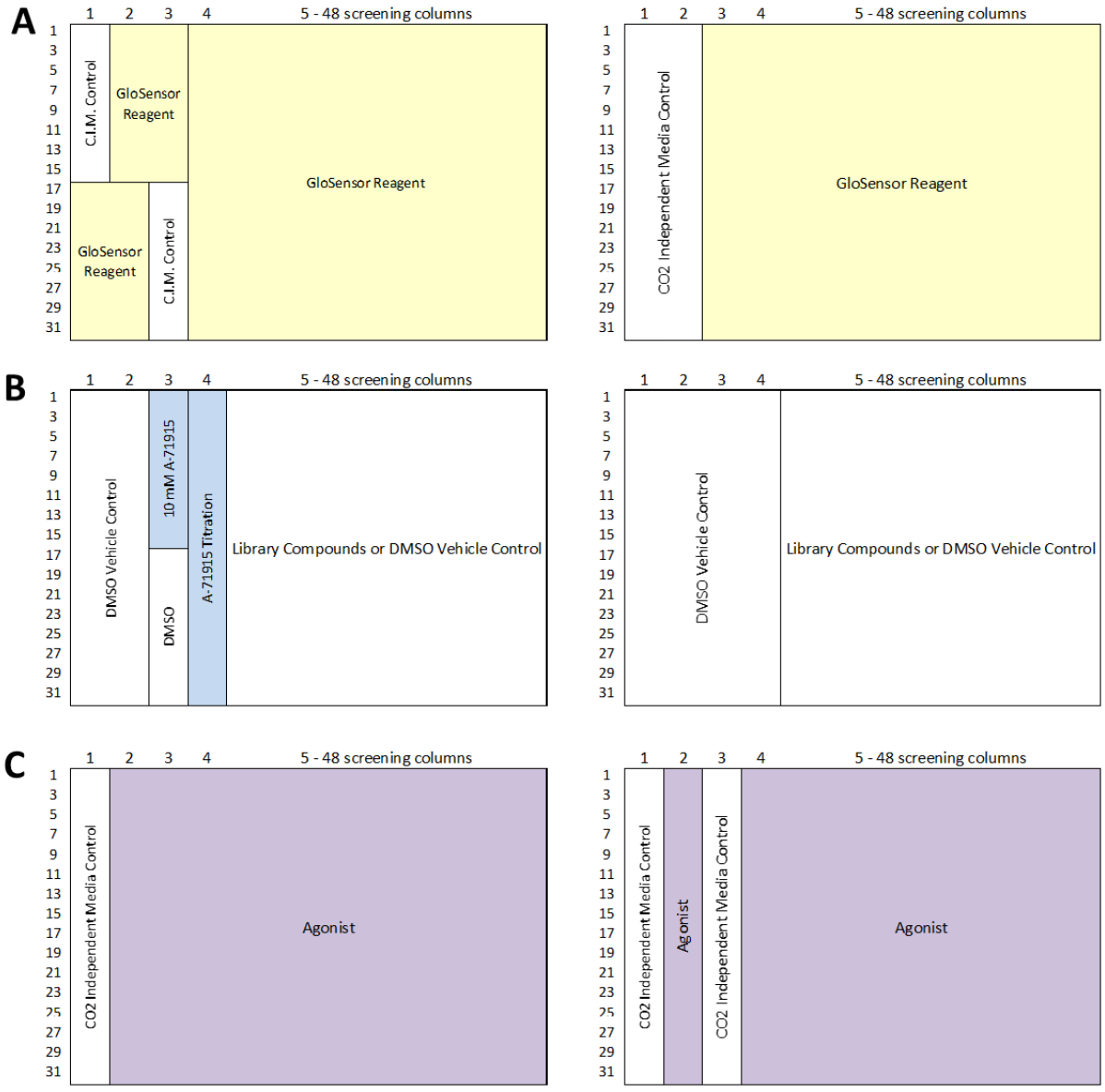
A
1 2 3 4 5 - 48 screening columns
C.I.M. Control
GloSensor Reagent
GloSensor Reagent
GloSensor Reagent
C.I.M. Control
GloSensor Reagent
1 2 3 4 5 - 48 screening columns
CO2 Independent Media Control
GloSensor Reagent
B
1 2 3 4 5 - 48 screening columns
DMSO Vehicle Control
10 mM A-71915
DMSO
A-71915 Titration
Library Compounds or DMSO Vehicle Control
1 2 3 4 5 - 48 screening columns
DMSO Vehicle Control
Library Compounds or DMSO Vehicle Control
C
1 2 3 4 5 - 48 screening columns
CO2 Independent Media Control
Agonist
1 2 3 4 5 - 48 screening columns
CO2 Independent Media Control
Agonist
CO2 Independent Media Control
Agonist

Fig. S8. General plate map layout for qHTS. Plate layouts for GloSensor qHTS assays are given, hNPR1-expressing cells on the left and hNPR2-expressing or parental HEK-cGMP-sensor cells on the right. (A) 16-24 h after plating of cells, 1 μl GloSensor reagent (yellow background) or CO_2 independent media (C.I.M.) as a control (white background) was added to respective wells. (B) 2 h after addition of GloSensor reagent, library compounds or DMSO (white wells) were pinned into plates. The control compound A-71915 was only added to HEK-hNPR1-cGMP-sensor cells (blue wells). The final concentration of A-71915 added to rows 1-16 of column 3 was 38.3 μM, whereas a 16-pt A-71915 titration ranging from a final concentration of 38.3 μM down to 1.2 nM was added in duplicate to column 4. (C) 30-60 minutes after compound addition, 1 μl of respective agonist (purple columns) or CO_2 independent media as a control (white columns) was dispensed to designated wells. Final concentrations were 0.1 nM for hNPPA (HEK-hNPR1-cGMP-sensor cells) and NPPC (HEK-hNPR2-cGMP-sensor cells), or 50 μM for SNP (HEK-cGMP-sensor cells).

Figure S9

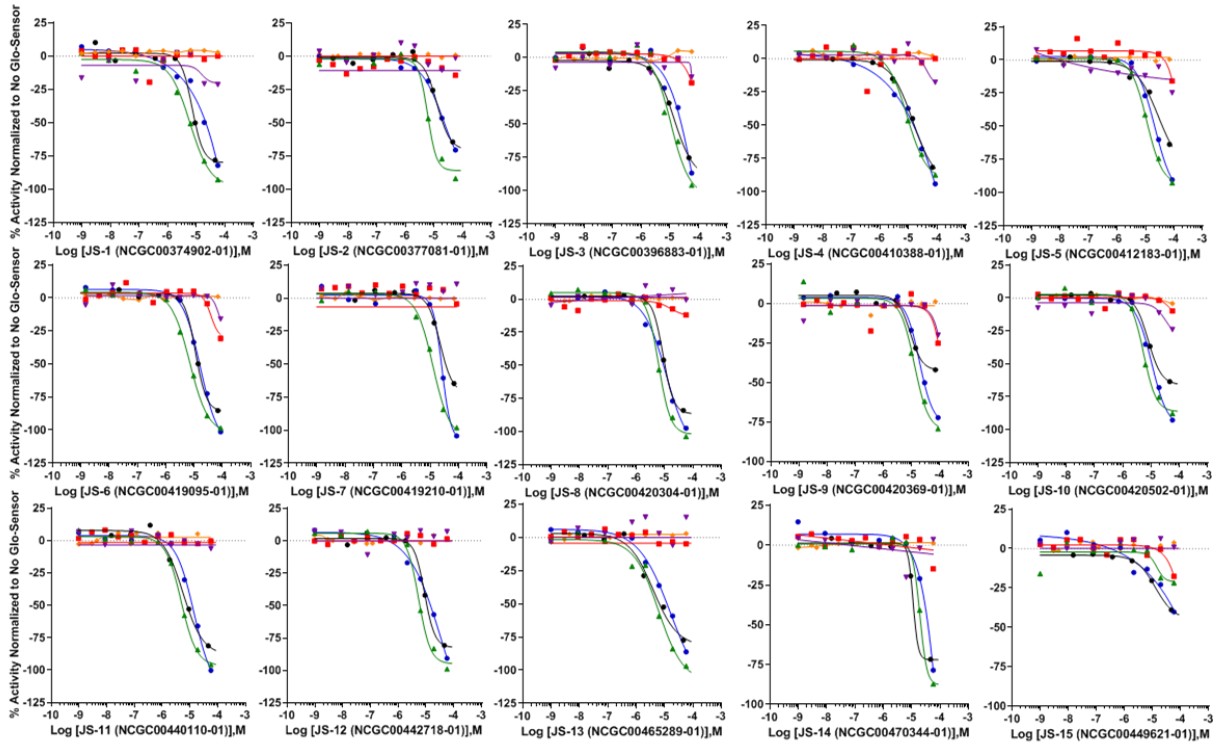

Fig. S9. qHTS concentration response curves for JS-1 through JS-15. (●) HEK-hNPR1-cGMP-sensor cell line concentration response curves (CRC) from primary Genesis library qHTS. (●) HEK-hNPR1-cGMP-sensor cell line CRC from follow-up reconfirmation qHTS. (▲) HEK-hNPR2-cGMP-sensor cell line CRC from follow-up qHTS. (▼) HEK-cGMP-sensor cell line CRC from follow-up qHTS. (♦) *Firefly* luciferase enzymatic inhibition CRC from follow-up qHTS. (■) HEK-hNPR1-cGMP-sensor cell line CellTiter-Glo cytotoxicity CRC from follow-up qHTS. Data are single determinations obtained from PubChem AIDs: 1347048 (●); 1347044 (●); 1347046 (▲); 1347051 (▼); 1347047 (♦); 1347044 (■), plotted in Prism 7.0 using 4-parameter logistic fits.

Table S1. Summary of qHTS and counterscreens.

Summary of data obtained from follow-up screening. Lipophilicity was estimated in silico by calculating MlogP, using the method of Moriguchi (72). The apparent potency (IC_{50}) and efficacy (I_{max}) in five different assays for each candidate compound is tabulated: Inhibition of hNPPA-stimulated HEK-hNPR1-cGMP-sensor cells, inhibition of NPPC-stimulated HEK-hNPR2-cGMP-sensor cells, inhibition of SNP-stimulated HEK-cGMP-sensor cells, inhibition of *Firefly* luciferase in vitro, and cytotoxicity on HEK-hNPR1-cGMP-sensor cells. Concentration-response-curve in each assay was fit with a four-parameter logistic regression. For counter-screens, potency and efficacy of compounds frequently could not be determined as fits did not converge (n. c.) and inhibition was not detectable at all (n. d.), respectively.

NCGC number	**given name**	**MlogP**	**HEK-hNPR1-cGMP-sensor cells**		**HEK-hNPR2-cGMP-sensor cells**		**HEK-cGMP-sensor cells**		**Fluc in vitro**		**cytotoxicity**	
			IC_{50} [µM]	**I_{max} [%]**	**IC_{50} [µM]**	**I_{max} [%]**	**IC_{50} [µM]**	**I_{max} [%]**	**IC_{50} [µM]**	**I_{max} [%]**	**IC_{50} [µM]**	**I_{max} [%]**
00374902-01	JS-1	3.238	26 ± 1.5	-119 ± 20	7.2 ± 1.3	-106 ± 8	n. c.	n. d.	0.03 ± 1.5	-3 ± 3	n. c.	n. d.
00377081-01	JS-2	4.132	25 ± 1.3	-102 ± 9	6.4 ± 1.1	-88 ± 5	n. c.	n. d.	n. c.	n. d.	n. c.	n. d.
00396883-01	JS-3	3.001	62 ± 19	-183 ± 67	17 ± 20	-126 ± 23	n. c.	n. d.	25 ± 4	-1 ± 6	n. c.	n. d.
00410388-01	JS-4	2.767	16 ± 13	-110 ± 10	11 ± 1.2	-100 ± 5	n. c.	n. d.	n. c.	n. d.	n. c.	n. d.
00412183-01	JS-5	3.999	32 ± 13	-127 ± 12	12 ± 1.1	-97 ± 4	n. c.	n. d.	n. c.	n. d.	n. c.	n. d.
00419095-01	JS-6	2.332	24 ± 1.2	-15 ± 3	6.9 ± 1.1	-102 ± 3	n. c.	n. d.	n. c.	n. d.	45 ± 43	-36 ± 87
00419210-01	JS-7	1.954	85 ± 22	-216 ± 97	16 ± 1.3	-122 ± 11	n. c.	n. d.	n. c.	n. d.	n. c.	n. d.
00420304-01	JS-8	3.238	13 ± 1.2	-122 ± 9	9.1 ± 1.4	-127 ± 13	n. c.	n. d.	n. c.	n. d.	49 ± 14	-22 ± 29

00420369-01	JS-9	1.118	35 ± 15	-106 ± 18	20 ± 16	-102 ± 16	n. c.	n. d.	n. c.	n. d.	n. c.	n. d.
00420502-01	JS-10	1.366	17 ± 1.3	-122 ± 12	5.4 ± 1.4	-86 ± 5	n. c.	n. d.	n. c.	n. d.	n. c.	n. d.
00440110-01	JS-11	4.132	21 ± 1.3	-140 ± 13	5.0 ± 1.1	-97 ± 4	n. c.	n. d.	n. c.	n. d.	n. c.	n. d.
00442718-01	JS-12	3.555	16 ± 1.3	-116 ± 11	5.7 ± 1.1	-96 ± 4	n. c.	n. d.	n. c.	n. d.	n. c.	n. d.
00465289-01	JS-13	3.936	10 ± 1.2	-99 ± 6	5.9 ± 1.3	-108 ± 8	n. c.	n. d.	n. c.	n. d.	n. c.	n. d.
00470344-01	JS-14	3.001	117 ± 75	-286 ± 966	20 ± 1.1	-91 ± 8	n. c.	n. d.	n. c.	n. d.	n. c.	n. d.
00449621-01	JS-15	2.961	6.9 ± 2.0	-41 ± 8	41 ± 13.8	-41 ± 8	n. c.	n. d.	n. c.	n. d.	n. c.	n. c.

Table S2. Corroboration of hNPR1 inhibition in screening assay.

HEK-hNPR1-cGMP-sensor cells were seeded in 96-wells and stimulated with 60 pM hNPPA 5 minutes after addition of candidate compounds or A-71915 and luminescence was measured for 30 minutes. Inhibitors were titrated to calculate apparent potency (IC_{50}) and efficacy (I_{max}) of inhibition of hNPPA-induced cGMP production.

given name	IC_{50} [µM] (mean ± SEM)	I_{max} [%] (mean ± SEM)
JS-3	3.1 ± 0.6	-99.4 ± 0.6
JS-4	1.1 ± 0.01	-95.5 ± 1.2
JS-5	7.4 ± 0.3	-99.9 ± 0.1
JS-6	1.9 ± 0.1	-94.2 ± 5.3
JS-7	1.2 ± 0.5	not determined
JS-8	1.2 ± 0.1	-98.8 ± 0.7
JS-9	3.1 ± 1.4	-93.4 ± 6.4
JS-10	6.7 ± 6.7	-98.3 ± 1.7
JS-11	1.9 ± 0.8	-96.3 ± 1.3
JS-12	1.3 ± 0.002	-96.0 ± 1.3
JS-13	1.1 ± 0.1	-96.1 ± 0.4
JS-14	3.1 ± 1.1	not determined
A-71915	1.1 ± 0.1	-99.8 ± 0.1

Table S3. SafetyScreen44-dependent test for off-targets of JS-11.

SafetyScreen44 was used to identify potential off-target effects of JS-11. Each target was tested for inhibition by 10 μM JS-11 in duplicate by Eurofins Panlabs Discovery Services Taiwan. Significant inhibition (*) of a target was accepted for ≥ 50% inhibition.

gene	agonist or substrate	quantitation method	inhibition (%)
ACHE	Acetylthiocholine	Spectrophotometry of thiocholine	10
PTGS1	Arachidonic acid	EIA of PGE_2	-9
PTGS2	Arachidonic acid	EIA of PGE_2	1
MAOA	Kynuramine	Spectrophotometry of 4-hydroxyquinoline	0
PDE3A	FAM-cAMP	Fluorescein-AMP IMAP	9
PDE4D2	FAM-cAMP	Fluorescein-AMP IMAP	20
LCK	Poly(Glu:Tyr) + $[^{32}P]$-ATP	$[^{32}P]$-Poly(Gly:Tyr) quantitation	1
ADORA2A	$[^{3}H]$ CGS-21680	Radioligand binding	15
ADRA2A (rat submaxillary gland)	$[^{3}H]$ Prazosin	Radioligand binding	12
ADRA2A	$[^{3}H]$ Rauwolscine	Radioligand binding	27
ADRB1	$[^{121}I]$ Cyanopindolol	Radioligand binding	-4
ADRB2	$[^{3}H]$ CGP-12177	Radioligand binding	7
AR	$[^{3}H]$ Methyltrienolone	Radioligand binding	6
L-type calcium channel (rat cerebral cortex)	$[^{3}H]$ Nitrendipine	Radioligand binding	2
CNR1	$[^{3}H]$ SR141716A	Radioligand binding	19
CNR2	$[^{3}H]$ WIN-55,212-2	Radioligand binding	3
CCKAR	$[^{125}I]$ CCK-8	Radioligand binding	82*
DRD1	$[^{3}H]$ SCH-23390	Radioligand binding	-2
DRD2 (short isoform)	$[^{3}H]$ Spiperone	Radioligand binding	7
EDNRA	$[^{125}I]$ Endothelin-1	Radioligand binding	-3
$GABA_A$ receptor (rat brain w/o cerebellum)	$[^{3}H]$ Flunitrazepam	Radioligand binding	22
NR3C1	$[^{3}H]$ Dexamethasone	Radioligand binding	11
NMDA-type glutamate receptor (rat cerebral cortex)	$[^{3}H]$ CGP-39653	Radioligand binding	-7
HRH1	$[^{3}H]$ Pyrilamine	Radioligand binding	-3
HRH2	$[^{125}I]$	Radioligand binding	-3

	Aminopotentidine		
CHRM1	[^{3}H] N-Methylscopolamine	Radioligand binding	-3
CHRM2	[^{3}H] N-Methylscopolamine	Radioligand binding	-15
CHRM3	[^{3}H] N-Methylscopolamine	Radioligand binding	-17
CHRNA4/B2 ($\alpha4_2\beta2_3$)	[^{3}H] Cytisine	Radioligand binding	3
OPRD1	[^{3}H] Naltrindole	Radioligand binding	-1
OPRK1	[^{3}H] Diprenorphine	Radioligand binding	26
OPRM1	[^{3}H] Diprenorphine	Radioligand binding	16
A-type potassium channel (rat cerebral cortex)	[^{125}I] α-Dendrotoxin	Radioligand binding	-3
KCNH2	[^{3}H] Dofetilide	Radioligand binding	2
HTR1A	[^{3}H] 8-OH-DPAT	Radioligand binding	10
HTR1B	[^{3}H] GR125743	Radioligand binding	9
HTR2A	[^{3}H] Ketanserin	Radioligand binding	83*
HTR2B	[^{3}H] Lysergic acid diethylamide	Radioligand binding	49
HTR3	[^{3}H] GR-65630	Radioligand binding	-5
Voltage-gated sodium channel (rat brain)	[^{3}H] Batrachotoxinin	Radioligand binding	-9
SLC6A3	[^{125}I] RTI-55	Radioligand binding	13
SLC6A2	[^{125}I] RTI-55	Radioligand binding	4
SLC6A4	[^{3}H] Paroxetine	Radioligand binding	6
AVPR1A	[^{125}I] Phenylacetyl-Y(Me)FQNRPRY	Radioligand binding	-9

Table S4. Inhibition of hNPR1 in membrane cyclase assay.

Summary of data collected for the cell-free NPR1 membrane cyclase assay. Membranes were stimulated with 1 nM hNPPA with and without titrations of candidate compounds and A-71915. Potency (IC_{50}) and efficacy (I_{max}) of inhibition of hNPPA-induced cGMP production were calculated as described in methods.

given name	IC_{50} [µM] (mean ± SEM)	I_{max} [%] (mean ± SEM)
JS-3	4.0 ± 1.2	-98.2 ± 1.8
JS-4	2.8 ± 0.04	-96.1 ± 3.7
JS-5	0.1 ± 0.1	-99.8 ± 0.1
JS-6	0.8 ± 1.9	-99.4 ± 0.5
JS-7	0.1 ± 0.3	-98.4 ± 1.5
JS-8	0.3 ± 0.4	-98.0 ± 2.0
JS-9	2.2 ± 1.8	-95.3 ± 4.5
JS-10	0.7 ± 0.6	-95.2 ± 3.3
JS-11	1.4 ± 0.1	-99.7 ± 0.2
JS-12	0.7 ± 0.1	-99.0 ± 1.0
JS-13	0.8 ± 0.9	-94.4 ± 5.4
JS-14	12.7 ± 4.9	-99.0 ± 0.0
A-71915	0.1 ± 0.03	-98.0 ± 3.5

Table S5. K_i values for hNPR1 and mNPR1.

Summary of IC_{50} data from tables S2, S4, and S6 were used to calculate the inhibitor constant K_i, using the Cheng-Prusoff equation ($K_i = \frac{IC_{50}}{1+\frac{[NP]}{EC_{50}}}$). K_i values between different assays and receptors were compared with 2-way ANOVA and Tukey's multiple comparisons post-hoc test or unpaired t-test (JS-7). Only the K_i for JS-6 was significantly higher at mNPR1 compared to hNPR1 (GloSensor, p = 0.0423; cyclase assay, p = 0.0253) whereas the K_i for JS-14 in the hNPR1 cyclase assay was significantly higher compared to both GloSensor assays (hNPR1, p = 0.0001; mNPR1, p < 0.0001).

given name	K_i hNPR1 GloSensor [µM] (mean ± SEM)	K_i hNPR1 cyclase assay [µM] (mean ± SEM)	K_i mNPR1 GloSensor [µM] (mean ± SEM)
JS-3	0.50 ± 0.102	0.97 ± 0.295	0.25 ± 0.036
JS-4	0.18 ± 0.002	0.68 ± 0.010	0.22 ± 0.070
JS-5	1.18 ± 0.048	0.03 ± 0.033	0.42 ± 0.265
JS-6	0.31 ± 0.023	0.19 ± 0.455	1.69 ± 1.395*
JS-7	0.19 ± 0.085	0.03 ± 0.072	not determined
JS-8	0.20 ± 0.013	0.08 ± 0.107	0.10 ± 0.006
JS-9	0.49 ± 0.215	0.53 ± 0.434	0.57 ± 0.0004
JS-10	1.07 ± 1.079	0.18 ± 0.149	0.31 ± 0.037
JS-11	0.30 ± 0.134	0.34 ± 0.013	0.10 ± 0.030
JS-12	0.21 ± 0.0002	0.16 ± 0.024	0.26 ± 0.006
JS-13	0.18 ± 0.011	0.19 ± 0.214	0.21 ± 0.046
JS-14	0.50 ± 0.179	3.09 ± 1.197*	0.32 ± 0.329
A-71915	0.18 ± 0.016	0.04 ± 0.007	0.05 ± 0.005

Table S6. hNPR1 antagonists also inhibit mNPR1.

HEK-293 cells transiently expressing mNPR1 and pGS-40F were stimulated with 1 nM mNPPB 5 minutes after addition of candidate compounds or A-71915 and luminescence was measured for 30 minutes. Inhibitors were titrated to calculate apparent IC_{50} values, as described in methods.

given name	IC_{50} [µM] (mean ± SEM)
JS-3	12 ± 1.8
JS-4	11 ± 3.4
JS-5	20 ± 12
JS-6	82 ± 68
JS-8	4.7 ± 0.3
JS-9	28 ± 0.02
JS-10	15 ± 1.8
JS-11	4.9 ± 1.5
JS-12	13 ± 0.3
JS-13	10 ± 2.2
JS-14	15.8 ± 16
A-71915	2.2 ± 0.3

Table S7. In vitro pharmacokinetics of JS-11 and JS-8.

Basic pharmacokinetic parameters of JS-8 and JS-11 were determined in vitro (see methods for details).

given name	kinetic solubility assay [µg/ml]	rat liver microsome stability assay half-life [min]	PAMPA [cm/sec]
JS-8	< 1	1.41	964×10^{-6}
JS-11	15.64	12.37	1124×10^{-6}

Table S8. PubChem AIDs deposited and used for this study.

No.	Stage	Assay	PubChem AID
1	Assay validation	LOPAC test with HEK-cGMP-sensor cells	1347045
2	Assay validation	LOPAC test with HEK-hNPR1-cGMP-sensor cells	1347049
3	Assay validation	LOPAC test with HEK-hNPR2-cGMP-sensor cells	1347050
4	Primary qHTS	Genesis library qHTS with HEK-hNPR1-cGMP-sensor cells	1347048
5	Selection of follow-up compounds	*Firefly* luciferase inhibitor database (Genesis library)	1347043
6	qHTS follow-up	1,408 Genesis compounds tested in HEK-hNPR1-cGMP-sensor cells	1347044
7	qHTS follow-up	1,408 Genesis compounds tested in HEK-cGMP-sensor cells	1347051
8	qHTS follow-up	1,408 Genesis compounds tested in *Firefly* luciferase enzymatic assay	1347047
9	qHTS follow-up	1,408 Genesis compounds tested in HEK-hNPR1-cGMP-sensor cells for cytotoxicity	1347044
10	qHTS follow-up	1,408 Genesis compounds tested in HEK-hNPR2-cGMP-sensor cells	1347046

Table S9. Clinical information of human DRG donors.

DRG tissue was obtained from Tissue For Research (donor 1 and 2) and the NIH NeuroBioBank (donor 3-6). Spinal cord total RNA (donor 3, 7-9) was also obtained from the NIH NeuroBioBank. Basic clinical data for each donor are summarized.

donor ID	age	gender	race	cause of death	use
1	42	female	white	chronic inflammatory demyelinating polyneuritis	ISH
2	68	male	white	chronic obstructive pulmonary disease	ISH
3	48	male	black	congestive heart failure	ISH + qPCR
4	41	male	white	atherosclerosis	ISH
5	22	female	white	motor accident	qPCR
6	39	female	white	congestive heart failure	qPCR
7	41	male	black	pulmonary thromboembolism	qPCR
8	50	male	white	acute alcohol intoxication	qPCR
9	45	male	white	acute hemopericardium	qPCR

Data file S1. LOPAC pilot screening data. (data no. 1-3 from Table S8 were compiled in one Excel file)

Data file S2. Genesis primary qHTS screening data. (data no. 4 from Table S8 is given as an Excel file)

Data file S3. qHTS follow-up screening data. (data no. 6-10 from Table S8 were compiled in one Excel file)

Data file S4. Raw data. (provided as a separate Excel file)